A Millimeter λ Phase Stability Analysis of the South Baldy and Springerville Sites

M.A. Holdaway

November 22, 1991

1 Abstract

Site testing for the Millimeter Array has been underway at South Baldy, NM for about four years and at Springerville, AZ for about two. In addition to opacity measurements, the tipping radiometers at each site have performed stability measurements at 230 GHz which yield the Allan standard deviation at various averaging times of the sky brightness temperature fluctuations. The Allan standard deviation is related to the phase structure function $D_\phi(\rho)$ if the velocity is known (Treuhoft and Lanyi, 1987), so in principle we could take the Allan standard deviation "profiles" and determine the behavior of an interferometer of baseline ρ. The details of this problem do not lend themselves to an analytic solution, so we have turned to computer simulations.

The simulations indicate that South Baldy is a better 1 mm site than Springerville. At 230 GHz, the two sites are comparable in the most compact configuration and in the large configurations when selfcalibration is possible. When selfcalibration is not an option, phase stable interferometry in the A and B configurations would be possible at South Baldy between 10% and 20% of the winter time. At Springerville, phase stable observing in the two large arrays would be very rare.

2 The Data

2.1 *A priori* Information

The first piece of data we have is really a piece of belief: the turbulent atmosphere has a Kolmogorov power spectrum. A Kolmogorov power spectrum will lead to a phase structure function which varies with baseline length as $\rho^{5/3}$ for ρ less than the width of the turbulent layer, and $\rho^{2/3}$ for ρ greater than the turbulent layer (slopes of 5/6 and 1/3 in the rms phase variations over a sufficiently large time). Bester et al see a spectrum of ρ^1 (a random power spectrum in the phase fluctuations) over baselines of 10 m

at infrared wavelengths during conditions of excellent atmospheric stability. Also, the interferometric phase stability measurements of Sramek (1989) with the VLA indicate that the break from 5/3 to 2/3 power laws occurs on baselines less than 1 km. When the atmospheric data are ambiguous, we will rely upon this *a priori* information for guidance.

2.2 Wind Velocity and Height of the Turbulent Atmosphere

The velocity of the turbulent layer and the height above the array of the turbulent layer are needed to run the simulation program. Surface wind velocity data was taken concurrently with the atmospheric stability data at the two sites. During the very best observing conditions, surface wind velocities at both sites are about 4 m/s. For other conditions, the average surface winds are about 7 m/s at South Baldy and about 2 m/s at Springerville. The low winds at Springerville are likely due to the local topography, but it seems that the generally high wind speeds at South Baldy suggest that South Baldy is reaching up into the jet stream. Hence, the low surface winds during the best conditions at South Blady suggest that these conditions may be produced by low wind speeds. The consequences of erroneous assumptions about the wind velocity will be discussed later.

The velocity of the pattern of turbulent water vapor is likely to be different from the surface wind velocity. Radiosonde measurements of wind velocities at 4200 m (about 1000 m above the array) have been averaged over the last 20 years for Albuquerque, NM and Winslow, AZ (Schwab, 1991). Also, the average velocity as a function of time of year has been determined at 3400 m, 4200 m, and 5000 m over 1 year for both radiosonde sites. The South Baldy MMA site is about 100 miles south of the Albuquerque radiosonde site, and the Springerville MMA site is about 100 miles SE of Winslow and 150 miles SW of Albuquerque. The median wind velocity at 4200 m for the months of November through February is about 12 m/s at Winslow and about 14 m/s at Albuquerque. Wind speeds increase by about 15% for every 800 m of elevation gain. Hence, the altitude of the turbulent layer is not critical for the stability simulations. A wind velocity of 12 m/s was used for all simulations presented here. The height of the turbulent layer above the array was taken to be 1000 m for most cases, with all exceptions noted explicitly.

2.3 Water Vapor Radiometer Data

The water vapor radiometers measure the total power emitted by the sky at zenith every 3.51 s for one hour. Since the unevenly mixed water vapor in the turbulent atmosphere leads to variations in the total power measured by the water vapor radiometer as well as the phase fluctuations in an interferometer, it should be possible to determine the latter from the former. A naive calculation indicates that

$$\Delta\phi \approx 150 \cdot \Delta T_B$$

(McKinnon, 1988), but it is unclear on what time scales ΔT_B is to be measured and on what baselines $\Delta\phi$ is applicable to. Such a treatment ignores the detailed shape of the distribution of power on various scales in the atmosphere, so a more complicated analysis must be used.

The stability data which we used consisted of the Allan standard deviation (square root of the Allan Variance) of the radiometer time series calculated for averaging times of $2^{n-1} \cdot 3.51$ s for n = 1 to 9. Nominally, this yields information about the atmospheric turbulence on scales ranging from 3.51 s · 12 m/s = 42 m to 898 s · 12 m/s = 11000 m. Weaknesses in the data at both ends of this range impair our ability to predict the phase stability for the shortest and longest baselines (see below), but the *a priori* information about the behavior of atmospheric turbulence sometimes enables us to extrapolate at both ends.

In the southwest United States, the winter months offer the lowest opacity and best atmospheric stability. Hence, the ASD profiles were compiled for the months of November, December, January and February of 1990-1991 for the South Baldy and Springerville sites. To improve the statistics of the profiles without introducing confusion among different atmospheric conditions, the Allan standard deviation profiles were binned by the value of the Allan standard deviation at 56 s averaging time. The number of stability runs which fell into each bin are summarized in Table 1, while the average Allan standard deviation profiles are plotted on a log-log plot in Figures 1 and 2. Each average Allan standard deviation profile is named by the upper limit of the Allan standard deviation at 56 s averaging time (the profile formed by averaging all profiles with 0.04 < ASD(56 s) < 0.07 is labeled by 0.07).

2.4 Relative Abundances of Atmospheric Conditions

Data were selected by opacity ($\tau < .2$) and stability (ASD(56 s)<0.30). For higher opacities, the atmosphere is not optically thin and the emission from higher altitudes would be partially absorbed by the water vapor at lower elevations, a complication we would rather not deal with at this point. For high ASD values, the atmospheric emission may include substantial amounts of water droplets, which requires a different physical model. These selection criteria eliminate half of the winter observing time. As the simulations will show, much of the time eliminated by these criteria will permit 3 mm and 9 mm observations in all configurations, as well as some 1 mm observing in the compact array.

Consider the amount of time during which the very best stability conditions occur at the two sites. Tables 1 and 2 indicate that both sites have approximately equal amounts of time with ASD(56 s) better than 0.30, 0.20, and even 0.13. However, South Baldy has almost twice as much time than Springerville better than 0.07, half of which is better than 0.04. Springerville has essentially no time with ASD(56 2) better than 0.04. So, if the meaning of the ASD(56 s) values are assumed to have the same meaning at the two sites under consideration, it is clear that South Baldy comes out ahead if ASD(56 s) less than 0.07 is required for a substantial fraction of the observations that could be made with the MMA. The results of the simulations will shed new light on this data in two ways. The simulations will indicate just what phase stability is associated with a given ASD(56 s). Also, due to the differing natures of the turbulence at the two sites, the simulations will show that the same value for ASD(56 s) at the two sites *doesn't lead to the same phase stability!*

2.5 The Measured Allan Standard Deviation Profiles

The two sites show very different Allan standard deviation profiles in Figures 1 and 2. Unreliable points (points in which the errors in the removal of the instrumental function are clearly greater than the ASD value) are set equal to the next suspected reliable value. The last ASD point (896 s averaging time) is not significant as it is the average of only two numbers. When plotted on an appropriately scaled log-log plot against averaging time, the Allan standard deviations show the same behavior as the square root of the phase structure function plotted against distance. The conversion from time to distance is accommodated by the velocity of the turbulent atmosphere.

The best conditions at South Baldy show a slope of 0.5, consistent with a random spectrum of atmospheric turbulence, while less stable conditions show a slope of 0.83 breaking to 0.33, consistent with a Kolmogorov spectrum of turbulence. Modeling the atmosphere at the Baldy site is fairly straightforward.

The best conditions at the Springerville site are consistent with a Kolmogorov spectrum of turbulence, but all other cases show a complicated three part power spectrum. For each stability bin, the values of ASD(56 s) are required by the selection process to be equal for the Baldy and the Springerville data. However, the ASD for both shorter and longer averaging times is higher in the Springerville profiles than the South Baldy profiles. This indicates that the phase stability at Springerville will be worse than at Baldy on the both the shortest and the longest baselines. The upturn at the three longest averaging times (224 s, 448 s, and 896 s) indicates that the phase stability will be dramatically worse at Springerville on ~2.5 km to 10 km baselines. (The ASD measurements have no information on baselines longer than 10 km, and the 10 km information may not be reliable.) Springerville would not be an appropriate site for an extended (baselines > 3 km) array. The high ASD on the shortest three averaging times indicates that the phases may be rather poor on baselines shorter than 200 m. Springerville's higher ASD numbers at small averaging times should be interpreted with caution. Generally, they do not display the 0.83 power law slope ascribed to Kolmogorov turbulence. The error in the instrumental function subtraction is greater than the true atmospheric signal for the shortest averaging times at the best conditions. However, even at the worst conditions where such an error would be dominated by the true signal, the ASD profile remains flat for small averaging times suggesting that this behavior is true. Finally, while the radiometers used to measure the time series at the two sites were virtually identical and produced virtually identical results when operated on the same site (Baldy), the calibrated Springerville data seems to be quantized. This effect shows up on the shortest averaging times on the best conditions. These caveats must be considered when the Springerville atmosphere is modeled.

2.6 Possible Causes of Differences in the Allan Standard Deviation Profiles

Even without the simulations to guide us, it is apparent that the strength of the turbulence is often lower at South Baldy (indicated by the percentage

of time very good stability occurs), and that the nature of the turbulence is quite different at the two sites (indicated by the shapes of the ASD profiles). The qualitative and quantitative differences in the turbulence above the two sites is likely due to the local topography at the sites. The Baldy site sits on the top of a 3200 m mountain which overlooks 2200 m plains to the west. There are no features higher than 2800 m for at least 100 km to the west/northwest, the direction from which good weather comes. There are no local features which would cause anomalous turbulence.

The Springerville site is on a high plateau at 2900 m. A series of high mountains ranging from 3100 to 3500m sit 30 km to the west and northwest of the site. As the weather blows in from the west or northwest, these local features could generate large scale (>10 km) turbulent eddies. The excess power at long averaging times of the ASD could be due to transfer of power from the largest scale turbulence down to ~1 km eddies. Such large scale turbulence would not die out in the vicinity of the site where the stability measurements were taken, *ie*, all three of the sites which are topographically and politically feasible in this area would be adversely affected. On the other hand, the short averaging time or small spatial scale anomaly seen in the Springerville ASD profiles could be due to a local feature within a few hundred meters of the location of the measurements. If this were the case, the other two possible sites may not be affected. In the event that the Baldy site were ruled out, stability testing at the second Springerville site and the Alpine site would be important to determine if ant site in the area does not have problems on the short spacings.

3 The Simulation Program

We have undertaken a simple suite of atmospheric simulations which can relate the observed Allan standard deviations (ASD) to the interferometer phase fluctuations on various baselines and time scales.

- First, a model atmosphere is generated with the program ATMOMAKE. As will be explained later, this model atmosphere is chosen to be consistent with some observed Allan standard deviation profile in strength of turbulence and the relative amounts of power on various scales. The model atmosphere is a two dimensional representation of a three dimensional turbulent layer. The units of the pixel values are "millimeters of precipitable water vapor". The atmosphere is the Fourier transform of $\sqrt{F_\phi(\kappa)} \sim \kappa^{-\alpha}$, where $F_\phi(\kappa)$, the two dimensional

spectral power density, is defined by Tatarski (1961) as

$$D_\phi(\rho) = 4\pi \int_0^\infty (1 - J_\circ(\kappa\rho)) F_\phi(\kappa)\kappa d\kappa. \quad (1)$$

Input parameters to ATMOMAKE include inner and outer scale lengths of the atmospheric turbulence, a two part broken power law for $\sqrt{F_\phi(\kappa)}$ and the scale at which the power laws switch over, and the strength of the turbulence. In a three dimensional atmosphere, $D_\phi(\rho)$ will have a kinked power law form due to a change from 3-D turbulence on short spacings to 2-D turbulence on long spacings. The kink in the 2-D model atmosphere's spectrum serves to simulate this effect.

- Next, the program ATMOPHAS simulates a water vapor radiometer and an array of antennas observing a geostationary point source through the atmospheric phase screen moving with constant velocity. The atmosphere is in the near field of the interferometric elements, and the near field radiation pattern is assumed to be a cylinder which samples the atmosphere above each antenna in the direction of the source. Antenna based phase errors

$$\Delta\phi = 6.5 \frac{2\pi}{\lambda} \frac{mm_{H_2O}}{1000}$$

are introduced here. The atmosphere is in the far field of the radiometer and an Airy disk samples the atmosphere, measuring $(1-e^{-\tau})T_{sky}$, where $\tau = .06$ times the column density of water in millimeters. Input parameters of the ATMOPHAS program include T_{sky} (253 K), the atmospheric height, the atmospheric velocity (12 m/s), the observing frequency (230 GHz), the declination (the point source is essentially frozen at transit for the entire observation), and the length of the observation (1024 scans of 3.51 s). The output of the ATMOPHAS program consists of a time series from the radiometer, from which the Allan standard deviation profile can be calculated, and a visibility database which lists the complex visibilities as a function of baseline and time.

- The visibilities are processed by the PHRMS program. Here, the phases are "rewound" and binned by some time interval. The RMS of all phases about the mean within each time interval is calculated for each baseline and a range of binning times ranging from 30 s to

3600 s. Assuming sufficient averaging has occurred (high enough velocity, long enough observation time), $\sqrt{D_\phi(\rho)}$ is approximated by the rms phase at maximum binning time (3600 s) as a function of baseline. The power law slopes and breaks in the power laws of $\sqrt{D_\phi(\rho)}$ are mimicked by the Allan standard deviation profile. In fact, if plotted on the correct scale, the power laws are the same for the two. If the velocity is known, the breaks in the power laws show very good correspondence as well. This allows us to say something immediately about the atmosphere simply by looking at the raw Allan standard deviations.

A test of the simulation method will be carried out by comparing the simulated interferometer phases derived from Allan standard deviation profiles taken with a radiometer at the VLA site with concurrent VLA data. Twenty four such concurrent observations were taken in the winter of 1988-1989, but the data have not yet been analyzed with the methods presented here. The results of this investigation will be written up as a separate MMA memo.

4 Simulation Results

A trial and error process guided by numerically integrating Equation 1 leads us to the model parameters which describe an atmosphere which yields simulated Allan standard deviation profiles which are consistent with the measured (averaged) Allan standard deviation profiles. The simulated Allan standard deviation profiles are shown in Figures 3, 4, and 5. When the simulated and measured Allan standard deviations agree sufficiently in form and scale, the rms phases can be calculated for an arbitrary interferometer. Phase matrices which list the rms phase for several baselines and averaging times are presented for each model atmosphere studied (see Tables B, S1, and S2). Also, an example of $\sqrt{D_\phi(\rho)}$ for the BALDY.13 case is given in Figure 6. The short baseline slope is 0.81 and the long baseline slope is 0.40, consistent with the Kolmogorov values of 5/6 and 1/3. One point of interest is the turnover from 0.81 to 0.40. Sramek does not see this turnover in his VLA data, but it is clear that it does *not* exist in any data longer than 1000 m. There is a steepening of the rms phase to 0.59 for baselines less than 1000 m when all observations limited by the stability of the electronics are eliminated. Hence, the evidence is that the turnover occurs *somewhere*

below 1000 m, contrary to the conventional wisdom that the turnover occurs at 5000 m, the scale height of the turbulent troposphere. Our simulated structure function indicates the turnover occurs at only 250 m. The turnover could occur further out if our estimate for the velocity (12 m/s for South Baldy) is too low. The low turnover suggests that the thickness of the tropospheric turbulence is isolated to *thin* layers, on the order of 250 m think.

The atmospheric model which fit the South Baldy data is simple and is in line with the Kolmogorov theory. For 60 second averaging times for both the interferometer phase and the Allan standard deviation, the rms phase fluctuations on the longest spacings at South Baldy are more aptly described by

$$\Delta\phi = 200 \cdot \Delta T_{sky},$$

To fit the Springerville Allan standard deviation data at long averaging times, two independent atmospheric phase screens were used, one which generally agreed with the standard Kolmogorov theory, and one which had very little power on short scales and a steep power law on long scales, dominating the atmospheric fluctuations. There was no evidence for placing these two layers at different atmospheric heights or at different velocities (though this is by no means excluded by the data), so the standard values for the height (1000 m) and velocity (12 m/s) have been used. The short averaging time end of Springerville's Allan standard deviation profiles is not as steep as the Kolmogorov model and leads to greater phase fluctuations on short baselines. Because of potential problems with the measurement of the three shortest averaging times, two models for the atmosphere above Springerville have been produced. Springerville model 1, which actually agrees with the ASD data, shows poorer than expected phase stability on the shorter baselines. Springerville model 2 assumes a Kolmogorov model for short baselines, leading to lower phase fluctuations on the shorter baselines, and should be considered a "best case". Hence, if there is reason to doubt the short integration time ASD values, or if the small scale turbulence which causes the anomalously high ASD values at small integration times turns out to be local to the immediate area in which the radiometer data were obtained, then Springerville model 2 is more representative of what may be possible at the Springerville site.

A few points should be kept in mind:

- The last point on the Allan standard deviation plots is *not significant.* A bootstrap analysis of several simulations indicates that this point is in error by $\sim 25\%$.

- These simulations were performed with a linear array with wind velocity parallel to the array. Simulations with nonlinear arrays yield very similar results, with rms phases within about 20% of the phases computed for a linear array.

- These simulations were performed at the zenith. Phases must be multiplied by 1/ sin(elevation) to consider other declinations. For a source near the galactic center, this term is about 2.

- Before and after a source transits, the array will be observing through more airmass than at transit. It is assumed that MMA observations will proceed out to 1.4 times the transit airmass. Hence, in addition to the secant elevation term, the phases must be further multiplied by the average excess airmass due to change in elevation, about 1.2. Hence for a full integration on a source at δ = 35, the phases must be multiplied by 1.2, while for a source at δ = -25, the phases must be multiplied by 2.4.

4.1 Reliability of the Phase Stability Simulations

Short of a systematic error in the simulation programs or the radiometers, the simulations seem to be fairly robust by atmospheric standards. Phase stability on 1-3 km baselines is not very model dependent. Internal errors are less than 30% on these baselines. For the short baselines (< 200 m) at Springerville, the two models give results which differ by a factor of 2. As mentioned earlier, the altitude is not a critical parameter because the velocity changes slowly with altitude. Furthermore, the altitude has no effect on the simulated interferometer phases and only a minor effect on the simulated sky temperature fluctuations at short averaging times.

If the true velocity of the atmospheric phase pattern is significantly different from the assumed value of 12 m/s (as may be possible for the 0.04 bin on South Baldy), then the measured Allan standard deviation profiles indicate different phase stability than these simulations have produced. First, any kink in the phase structure function will move; a lower true velocity will cause the kink to move to smaller spatial scales. Since the 0.04 South Baldy ASD has no kink, this is not a problem. Second, since not as much atmosphere passes over the array, there will not be sufficient averaging on the longer baselines and the determined shape of the structure function will not be accurate. Third, to account for the the lower ASD in conjunction with the low velocity, the turbulence must be somewhat stronger than that

which is used in the model. These two effects, lower velocity and stronger turbulence, will approximately cancel out in both the ASD and the rms phases.

4.2 Interpretation of the Simulations

Looking at the phase stability for the worst atmospheric conditions included in this study ($0.20 < \mathrm{ASD}(56\ \mathrm{s}) < 0.30$), it is clear that 3 mm or 9 mm observations will have no problem at either the Baldy or Springerville sites. Even low elevation observations in the A array will present no problems at 3 mm if selfcalibration is possible. This means that the A array at either site will be usable for *at least* 50% of the winter time at frequencies of 100 GHz and lower. A better estimate of the time cannot be made given the selection criteria we have applied to the stability data. However, it is clear the A array will not sit around idle while waiting for the very best observing times to come around.

At 100 GHz, the two sites are quite comparable. At higher frequencies, we must look to better and better atmospheric conditions and we must consider both how good the atmosphere is at each site as well as how often these conditions occur.

Table 1 indicates the percent of time the ASD(56 s) is less than a given value at the Baldy and Springerville sites. However, in light of the fact that the same ASD(56 s) at Baldy and Springerville translate to different phase stabilities and the behavior with baseline is complicated, it is important to try to fold the simulation results back into the amount of time each condition range occurs at the two sites. In doing so, we will have a much better idea about what sorts of observations can be done and how often they can be done.

We estimate that interferometry will work with 30° rms phase errors. Observations of the galactic center at transit will have an airmass of two, so zenith phase fluctuations of 15° are required. For phase stable interferometry, we require the rms phase fluctuations over 3600 s to be less than or equal to 30° or 15°. On the other hand, if the target source is bright enough to detect on shorter times (selfcalibration is possible), then phase fluctuations of 30° or 15° over the detection time are acceptable. (For a 30 s integration time, a continuum source must be a few hundred mJy for selfcalibration to work.) These are the four cases we will examine: phase stable interferometry looking to the zenith and looking to the galactic center, and observations of strong sources which can be detected on each baseline in

30 s, looking to the zenith and to the galactic center.

The South Baldy model and the two Springerville models are considered in this light (the second Springerville model is the more optimistic). We know the fraction of time the ASD(56 s) falls into each bin, and we know the rms phase on the pertinent baselines and averaging times for the median atmosphere of each bin. It is assumed that the simulation results represent the median conditions of the corresponding bin. If we also assume that the occurrence of some phase fluctuation on some baseline is linear in time (cumulative time at which the atmosphere is better than that phase) between the midpoints of bins which straddle the phase in which we are interested (30° or 15°), a linear interpolation gives an estimate of the percent time the atmosphere will be better than that phase on that baseline.

Table 3 indicates the amounts of time interferometry would work if selfcalibration averaging times of 30 s were possible on 60 m, 210 m, 700 m, and 2000 m baselines, looking towards the galactic center and towards the zenith, at the Baldy and Springerville sites. These baselines were chosen because they are fairly long baselines in the D, C, B, and A arrays respectively, and will indicate how often observations in those arrays will succeed. Table 4 indicates the amounts of time phase stable interferometry would work on 60 m, 210 m, 700 m, and 2000 m baselines, looking towards the galactic center and towards the zenith, at the Baldy and Springerville sites. Interpolation errors are on the order of 1% as indicated by interpolation verses extrapolation. Errors inherent to the modeling procedure may contribute up to 3% as indicated by inconsistencies in Table 4, and for some portions of these tables, such as where the percentages are low and are dominated by the fraction of time given conditions occur, the errors will be much lower.

We draw the following conclusions from Tables 3 and 4:

- For zenith observations in which selfcalibration is possible, there is very little difference between the Baldy and Springerville sites.

- For zenith observations in which selfcalibration is possible, D array observations would be possible from both sites for all conditions which were not rejected by the selection criterion: selected D array observations will be possible *more than half of the winter observing period.*

- For higher airmass observations in which selfcalibration is possible, suitable atmospheric conditions exist roughly twice as often at Baldy than at Springerville.

- The most dramatic differences between the sites become evident when more difficult observations are considered. Phase stable observing in the A and B arrays at Springerville will be rare (except perhaps for looking overhead on 700 m baselines). The Baldy A and B arrays will be phase stable a reasonable amount of time (5% to 25%, depending upon the airmass and configuration).

While there is only a small amount of time at South Baldy which permits phase stable interferometry at 230 GHz in the A array, the stability data indicates that these good atmospheric conditions tend to last more than 5 hours (the time between consecutive stability measurements), sometimes lasting more than 24 hours but interrupted by unstable conditions in the afternoons.

Both sites are appropriate for 100 GHz work, for compact array work, and for work in which selfcalibration is a possibility, though Baldy is marginally better than Springerville for these observations. The most challenging experiments which require high resolution imaging of very weak sources appear to be possible only at the South baldy site.

Table 1: Number of stability measurements in each of the stability divisions at South Baldy and Springerville.

ASD(56 s) range	Baldy		Springerville	
<0.04	43	9.8%	5	1.1%
0.04 - 0.07	37	8.5%	41	9.0%
0.07 - 0.13	64	14.6%	89	19.6%
0.13 - 0.20	43	9.8%	60	13.2%
0.20 - 0.30	38	8.7%	32	7.0%
rejected	212	48.5%	227	50.0%

Table 2: Percentage of time at which the stability measurements are better than some value of the Allan standard deviation at 56 s.

ASD(56 s)	Baldy	Springerville
<0.04	9.8%	1.1%
<0.07	18.3%	10.1%
<0.13	33.0%	29.7%
<0.20	42.8%	43.0%
<0.30	51.5%	50.0%

Table 3: Percentage time at which rms phase error are less than 15° and 30° on 30 s integration times at South Baldy and Springerville. Selfcalibration required.

Baseline	15°			30°		
	B	S1	S2	B	S1	S2
60 m	40%	20%	34%	>52%	47%	>50%
210 m	26%	10%	14%	41%	31%	45%
700 m	26%	12%	15%	41%	34%	45%
2000 m	27%	11%	14%	43%	32%	44%

Table 4: Percentage time at which rms phase error are less than 15° and-30° on 3600 s integration times at South Baldy and Springerville. Phase stable.

Baseline	15°			30°		
	B	S1	S2	B	S1	S2
60 m	38%	18%	27%	>52%	44%	>50%
210 m	21%	7%	10%	36%	23%	30%
700 m	14%	2%	2%	26%	13%	16%
2000 m	6%	0%	0%	16%	2%	2%

Bester, M., Danchi, W.C., Degiacomi, C.G., Greenhil, L.J., and Townes, C.H., *Submitted to the Astrophysical Journal, 1991.*

McKinnon, Mark M. Measurement of Atmospheric Phase Stability with a 225 GHz Radiometer, MMA Memo 49. 1988.

Schwab, F. MMA Memo, *In preparation, 1991.*

Sramek, R. A. Atmospheric Phase Stability at the VLA, URSI/IAU Symposium on Radio Astronomical Seeing (1989).

Tatarski, V. I., Wave Propagation In A Turbulent Medium, McGraw-Hill, New York, 1961.

Treuhoft, R.N., and Lanyi, G.E. Radio Science, V 22, N 2 p. 251 1987.

Figure 1: Scaled log-log plot of the Allan standard deviation profiles from South Baldy, binned by conditions.

Figure 2: Scaled log-log plot of the Allan standard deviation profiles from Springerville, binned by conditions.

Figure 3: Simulated Allan standard deviation profiles for South Baldy.

Figure 4: Simulated Allan standard deviation profiles for Springerville, Model 1.

Figure 5: Simulated Allan standard deviation profiles for Springerville, Model 2.

Figure 6: Simulated phase structure function from one of the South Baldy model atmospheres.

BALDY.04.RMS.2

Baseline, m	Averaging Time, s 30.	60.	120.	240.	480.	960.	3600.
16.0	0.9	0.9	0.9	0.9	0.9	0.9	0.9
24.0	1.1	1.1	1.1	1.1	1.1	1.1	1.1
40.0	1.5	1.5	1.5	1.5	1.5	1.5	1.6
60.0	1.9	2.0	2.0	2.1	2.1	2.1	2.1
84.0	2.3	2.4	2.5	2.5	2.5	2.5	2.5
100.0	2.4	2.6	2.7	2.7	2.7	2.7	2.8
150.0	2.8	3.1	3.3	3.4	3.4	3.4	3.4
210.0	3.0	3.5	3.8	3.9	3.9	4.1	4.0
250.0	3.1	3.7	4.0	4.2	4.3	4.4	4.4
350.0	3.2	4.1	4.8	5.0	5.1	5.4	5.3
400.0	3.5	4.5	5.0	5.3	5.5	5.8	5.7
500.0	3.5	4.6	5.6	6.1	6.2	6.6	6.5
600.0	3.5	4.6	6.0	6.6	6.8	7.2	7.1
700.0	3.5	5.0	6.1	6.7	7.2	7.5	7.7
750.0	3.3	5.1	6.4	7.1	7.5	8.0	8.0
800.0	3.4	5.2	6.3	7.1	7.8	8.0	8.1
900.0	3.6	5.1	6.7	7.7	8.1	8.8	8.8
1000.0	3.5	4.9	6.8	8.0	8.5	9.3	9.3
1200.0	3.4	5.0	6.7	8.0	9.0	9.8	10.2
1400.0	3.4	4.8	6.7	8.5	9.5	10.7	11.0
1600.0	3.3	4.5	6.5	8.6	10.0	11.3	11.9
2000.0	3.3	5.2	6.9	9.2	11.5	12.6	13.5
2200.0	3.4	5.1	7.0	9.8	11.6	13.6	14.5
2400.0	3.3	5.0	6.9	9.9	12.4	14.2	15.2
3000.0	3.5	5.2	7.7	10.8	13.7	16.2	17.4

BALDY.07.RMS.2

Baseline, m	Averaging Time, s 30.	60.	120.	240.	480.	960.	3600.
	30.	60.	120.	240.	480.	960.	3600.
16.0	1.8	1.9	1.9	1.9	1.9	1.9	1.9
24.0	2.3	2.3	2.3	2.4	2.4	2.4	2.4
40.0	3.1	3.2	3.3	3.3	3.3	3.2	3.3
60.0	4.1	4.3	4.3	4.4	4.4	4.4	4.4
84.0	4.8	5.1	5.2	5.3	5.3	5.3	5.3
100.0	5.2	5.5	5.6	5.7	5.7	5.7	5.8
150.0	6.0	6.6	6.9	7.0	7.0	7.1	7.1
210.0	6.3	7.3	7.8	8.1	8.1	8.4	8.3
250.0	6.5	7.7	8.3	8.7	8.8	9.0	8.9
350.0	6.8	8.5	9.8	10.2	10.4	10.8	10.6
400.0	7.2	9.2	10.2	10.8	11.1	11.7	11.5
500.0	7.3	9.4	11.4	12.3	12.5	13.1	13.0
600.0	7.3	9.5	12.1	13.3	13.6	14.3	14.2
700.0	7.2	10.2	12.3	13.5	14.4	14.8	15.2
750.0	6.9	10.4	12.8	14.2	14.9	15.9	15.8
800.0	6.9	10.5	12.7	14.1	15.5	15.8	16.0
900.0	7.3	10.3	13.4	15.3	16.1	17.4	17.3
1000.0	7.3	10.0	13.6	15.9	16.8	18.2	18.2
1200.0	7.1	10.1	13.4	15.8	17.6	19.1	19.7
1400.0	7.1	9.8	13.3	16.7	18.6	20.7	21.3
1600.0	6.8	9.1	12.9	16.9	19.5	21.9	22.9
2000.0	6.9	10.4	13.8	18.1	22.1	24.2	25.8
2200.0	7.1	10.3	13.9	19.1	22.4	25.9	27.5
2400.0	6.8	10.0	13.7	19.2	23.9	27.1	28.9
3000.0	7.2	10.5	15.1	21.0	26.2	30.8	33.0

TABLE B

BALDY.13.RMS.2

Baseline, m	Averaging Time, s 30.	60.	120.	240.	480.	960.	3600.
16.0	3.3	3.5	3.5	3.6	3.6	3.6	3.6
24.0	4.2	4.5	4.6	4.6	4.6	4.6	4.6
40.0	6.0	6.5	6.6	6.6	6.7	6.6	6.6
60.0	8.1	8.7	8.9	9.0	9.0	8.9	9.0
84.0	10.3	11.3	11.5	11.7	11.7	11.7	11.7
100.0	11.3	12.6	12.8	13.0	13.1	13.0	13.0
150.0	13.8	15.7	16.3	16.6	16.7	16.6	16.7
210.0	15.2	18.1	18.9	19.4	19.6	19.5	19.5
250.0	15.4	19.1	20.2	20.8	21.0	21.0	21.0
350.0	14.6	19.0	21.4	22.5	23.2	23.6	23.4
400.0	14.2	20.3	22.4	23.0	23.9	24.7	24.1
500.0	14.1	20.5	23.4	24.9	26.0	26.8	26.4
600.0	14.3	21.5	24.6	26.5	27.8	28.9	28.2
700.0	15.7	20.9	24.9	27.1	28.0	29.6	29.3
750.0	14.2	19.0	24.6	26.8	29.3	30.5	29.9
800.0	15.1	20.2	25.3	27.8	28.1	30.0	29.8
900.0	14.3	19.1	24.4	27.3	30.5	31.8	31.3
1000.0	14.2	18.8	24.0	27.5	31.2	32.5	31.9
1200.0	14.4	19.1	23.9	28.2	30.5	33.9	33.6
1400.0	14.3	18.4	22.8	27.9	33.7	36.3	35.2
1600.0	13.7	17.9	22.6	28.5	33.5	38.2	37.1
2000.0	14.0	18.9	25.4	31.0	34.5	42.4	42.1
2200.0	15.4	19.5	24.7	32.1	40.4	45.4	44.7
2400.0	14.3	18.5	24.2	31.0	37.4	45.9	45.5
3000.0	13.8	19.5	23.4	31.7	42.0	50.7	50.6

BALDY.20.RMS.2

Baseline, m	Averaging Time, s 30.	60.	120.	240.	480.	960.	3600.
16.0	5.4	5.7	5.8	5.9	5.9	5.8	5.8
24.0	6.9	7.3	7.5	7.6	7.6	7.6	7.6
40.0	9.8	10.6	10.7	10.8	10.9	10.7	10.8
60.0	13.2	14.3	14.5	14.7	14.8	14.6	14.7
84.0	16.8	18.4	18.8	19.1	19.2	19.1	19.1
100.0	18.4	20.5	20.9	21.3	21.4	21.2	21.3
150.0	22.6	25.6	26.6	27.1	27.3	27.2	27.2
210.0	24.8	29.5	30.9	31.7	32.0	31.8	31.9
250.0	25.1	31.3	33.0	34.0	34.4	34.3	34.3
350.0	23.9	31.0	35.0	36.7	37.9	38.6	38.3
400.0	23.2	33.2	36.6	37.5	39.0	40.3	39.3
500.0	23.0	33.5	38.2	40.7	42.5	43.8	43.1
600.0	23.4	35.1	40.2	43.3	45.4	47.1	46.1
700.0	25.7	34.1	40.7	44.3	45.7	48.4	47.9
750.0	23.1	31.0	40.1	43.7	47.9	49.8	48.9
800.0	24.6	33.0	41.3	45.4	45.9	49.0	48.6
900.0	23.3	31.1	39.8	44.6	49.9	52.0	51.1
1000.0	23.2	30.8	39.2	44.9	50.9	53.1	52.1
1200.0	23.6	31.2	39.0	46.0	49.9	55.3	54.9
1400.0	23.3	30.1	37.3	45.6	55.1	59.2	57.5
1600.0	22.4	29.2	37.0	46.6	54.7	62.4	60.5
2000.0	22.9	31.0	41.5	50.7	56.3	69.3	68.7
2200.0	25.1	31.9	40.4	52.4	66.1	74.2	73.0
2400.0	23.3	30.3	39.6	50.7	61.0	74.9	74.4
3000.0	22.6	31.8	38.2	51.7	68.6	82.9	82.7

TABLE B

BALDY.30.RMS.2

Baseline, m	Averaging Time, s 30.	60.	120.	240.	480.	960.	3600.
16.0	8.3	8.7	8.8	8.9	8.9	8.8	8.9
24.0	10.5	11.2	11.4	11.5	11.5	11.5	11.5
40.0	14.9	16.1	16.3	16.5	16.5	16.3	16.5
60.0	20.1	21.7	22.0	22.3	22.5	22.2	22.4
84.0	25.5	28.0	28.6	29.0	29.1	29.0	29.0
100.0	28.0	31.2	31.8	32.4	32.6	32.2	32.4
150.0	34.3	39.0	40.5	41.2	41.5	41.3	41.4
210.0	37.7	44.9	47.0	48.2	48.6	48.4	48.5
250.0	38.2	47.5	50.1	51.6	52.3	52.2	52.2
350.0	36.3	47.2	53.2	55.9	57.6	58.7	58.2
400.0	35.3	50.5	55.6	57.1	59.4	61.4	59.8
500.0	34.9	50.9	58.2	61.9	64.6	66.7	65.5
600.0	35.6	53.3	61.1	65.8	69.1	71.7	70.1
700.0	39.0	51.8	61.9	67.4	69.4	73.6	72.9
750.0	35.2	47.1	61.0	66.5	72.8	75.8	74.4
800.0	37.5	50.2	62.8	69.1	69.8	74.6	73.9
900.0	35.5	47.4	60.6	67.9	75.9	79.0	77.6
1000.0	35.3	46.8	59.6	68.3	77.4	80.8	79.2
1200.0	35.8	47.5	59.3	69.9	75.8	84.1	83.5
1400.0	35.4	45.7	56.7	69.4	83.8	90.1	87.5
1600.0	34.0	44.4	56.2	70.9	83.2	94.8	92.0
2000.0	34.8	47.1	63.0	77.0	85.7	105.4	104.5
2200.0	38.1	48.4	61.4	79.7	100.4	112.8	111.0
2400.0	35.4	46.0	60.2	77.0	92.8	114.0	113.1
3000.0	34.4	48.3	58.1	78.7	104.3	126.0	125.7

TABLE B

SPRING.04.RMS.2

Baseline, m	Averaging Time, s 30.	60.	120.	240.	480.	960.	3600.
16.0	1.1	1.1	1.2	1.2	1.2	1.2	1.2
24.0	1.3	1.3	1.3	1.3	1.3	1.4	1.4
40.0	1.8	1.9	1.9	1.9	2.0	2.0	2.0
60.0	2.4	2.5	2.5	2.6	2.6	2.7	2.7
84.0	2.9	3.0	3.1	3.1	3.2	3.3	3.3
100.0	3.1	3.3	3.3	3.4	3.5	3.6	3.6
150.0	3.5	3.8	3.9	4.0	4.2	4.3	4.4
210.0	3.8	4.2	4.4	4.6	5.0	5.0	5.2
250.0	3.9	4.4	4.7	5.0	5.4	5.5	5.8
350.0	3.8	5.1	5.4	5.8	6.5	6.7	7.0
400.0	3.9	4.8	5.5	6.3	7.1	7.2	7.6
500.0	4.0	5.6	6.0	6.8	8.0	8.2	8.8
600.0	3.9	5.7	6.3	7.3	8.8	9.1	10.0
700.0	3.8	5.2	6.9	8.6	10.0	10.3	11.1
750.0	4.0	5.3	6.6	8.4	10.4	10.6	11.8
800.0	3.9	5.1	7.0	9.6	10.7	11.3	12.5
900.0	4.0	5.5	6.9	9.0	11.7	12.0	13.5
1000.0	4.0	5.7	7.1	9.4	12.5	13.0	14.6
1200.0	4.1	5.7	8.9	11.6	14.5	15.1	16.9
1400.0	4.1	6.1	8.6	11.5	15.9	16.6	19.1
1600.0	4.2	5.9	9.8	13.3	17.8	18.6	21.2
2000.0	4.2	6.2	9.7	15.8	20.6	22.1	25.3
2200.0	4.3	6.1	9.9	14.0	21.9	23.3	27.1
2400.0	4.2	6.4	10.5	16.7	23.3	25.1	29.0
3000.0	4.3	6.6	10.3	16.3	26.5	28.8	34.1

SPRING.07.RMS.2

Baseline, m	Averaging Time, s 30.	60.	120.	240.	480.	960.	3600.
16.0	2.8	2.9	2.9	3.0	3.0	3.0	3.0
24.0	3.5	3.7	3.7	3.7	3.7	3.8	3.8
40.0	5.0	5.2	5.2	5.3	5.3	5.4	5.3
60.0	6.6	6.9	7.1	7.2	7.2	7.3	7.2
84.0	7.9	8.4	8.5	8.7	8.8	8.9	8.7
100.0	8.6	9.2	9.4	9.6	9.7	9.8	9.6
150.0	9.6	10.6	11.1	11.5	11.6	11.8	11.6
210.0	10.5	12.1	12.9	13.4	13.6	13.7	13.6
250.0	10.7	12.6	13.6	14.2	14.5	14.5	14.6
350.0	10.8	13.7	15.2	16.3	16.8	16.9	17.1
400.0	10.7	13.9	15.7	16.8	17.4	17.4	18.0
500.0	10.2	13.6	16.2	17.8	18.7	18.9	19.6
600.0	10.0	13.3	16.6	18.7	19.9	20.1	21.1
700.0	10.0	14.1	17.4	19.5	21.4	21.4	22.6
750.0	10.1	14.1	17.3	20.1	21.8	22.4	23.8
800.0	10.1	14.2	18.5	21.0	21.6	22.6	23.7
900.0	10.0	13.9	17.3	20.9	23.1	24.3	25.9
1000.0	10.0	13.4	17.2	21.4	24.0	25.4	27.3
1200.0	9.9	13.9	17.9	21.3	26.3	27.3	29.6
1400.0	9.9	14.5	18.9	22.6	27.9	30.1	33.2
1600.0	10.5	14.3	19.3	22.4	29.8	31.4	35.3
2000.0	10.3	14.8	19.1	26.1	32.3	35.0	39.4
2200.0	10.6	15.0	19.8	23.4	34.6	37.3	43.1
2400.0	10.1	14.0	18.6	24.7	33.7	37.0	43.5
3000.0	10.0	14.3	18.9	24.5	37.6	41.6	50.5

TABLE 5 1

SPRING.13.RMS.2

Baseline, m	Averaging Time, s 30.	60.	120.	240.	480.	960.	3600.
16.0	6.6	6.8	6.9	7.0	7.0	7.0	6.9
24.0	8.4	8.7	8.7	8.7	8.8	9.0	8.8
40.0	11.9	12.2	12.2	12.3	12.3	12.6	12.3
60.0	15.7	16.1	16.4	16.5	16.6	16.8	16.4
84.0	18.4	19.1	19.3	19.6	19.6	19.9	19.5
100.0	19.7	20.6	20.9	21.2	21.2	21.5	21.0
150.0	21.4	23.0	23.6	24.1	24.2	24.6	24.0
210.0	22.3	24.9	25.9	26.5	26.7	26.9	26.5
250.0	22.2	25.3	26.6	27.3	27.6	27.6	27.5
350.0	21.8	26.4	28.5	29.8	30.3	30.5	30.4
400.0	21.7	26.7	29.0	30.4	31.0	30.9	31.3
500.0	20.6	25.8	29.2	31.1	32.0	32.0	32.7
600.0	20.1	25.1	29.5	31.9	33.1	33.1	34.2
700.0	20.4	26.4	30.6	33.1	35.3	34.9	36.3
750.0	20.6	25.9	30.4	33.7	35.5	36.0	37.5
800.0	20.7	26.6	31.6	34.9	35.5	36.5	37.4
900.0	20.5	25.8	30.3	34.4	36.8	38.2	39.8
1000.0	20.3	25.3	30.3	34.9	37.7	39.3	41.4
1200.0	20.2	25.6	30.6	34.8	40.6	41.9	44.3
1400.0	20.2	26.3	31.8	35.9	42.0	44.8	48.3
1600.0	21.1	26.2	32.0	35.8	44.6	46.4	51.1
2000.0	21.0	27.1	32.4	41.0	48.1	51.4	56.1
2200.0	21.3	27.6	33.5	37.2	50.6	53.9	60.8
2400.0	20.6	25.9	30.9	38.2	48.9	52.9	60.5
3000.0	20.4	26.0	31.6	37.9	53.5	58.3	69.0

SPRING.20.RMS.2

Baseline, m	Averaging Time, s 30.	60.	120.	240.	480.	960.	3600.
16.0	10.3	10.6	10.8	10.9	11.0	11.0	10.9
24.0	13.1	13.5	13.5	13.6	13.6	14.0	13.7
40.0	18.3	18.8	18.9	19.0	19.0	19.4	19.0
60.0	23.9	24.7	25.1	25.3	25.4	25.6	25.2
84.0	27.7	28.8	29.2	29.6	29.6	30.0	29.4
100.0	29.4	30.8	31.4	31.9	32.0	32.3	31.7
150.0	31.9	34.5	35.6	36.4	36.7	37.1	36.4
210.0	33.9	38.2	40.0	41.0	41.4	41.6	41.2
250.0	34.0	39.3	41.5	42.7	43.2	43.2	43.1
350.0	33.8	41.4	45.1	47.5	48.3	48.3	48.4
400.0	33.5	41.8	46.1	48.4	49.4	49.1	50.0
500.0	31.9	40.8	46.9	50.4	51.9	51.7	52.9
600.0	31.2	39.7	47.6	51.9	53.9	53.8	55.6
700.0	31.4	41.8	49.5	54.0	57.5	56.8	59.0
750.0	31.8	41.3	49.1	55.1	57.9	58.5	61.0
800.0	31.9	42.0	51.5	57.0	58.0	59.5	61.0
900.0	31.6	40.8	48.9	56.3	60.2	62.2	64.9
1000.0	31.3	39.9	48.7	57.1	61.7	64.2	67.5
1200.0	31.1	40.7	49.6	57.0	66.5	68.5	72.1
1400.0	31.2	41.9	51.7	59.3	69.0	73.4	78.8
1600.0	32.6	41.5	52.2	58.9	73.0	75.8	83.0
2000.0	32.3	43.0	52.3	67.3	78.7	83.7	90.6
2200.0	32.9	43.6	54.1	60.8	82.4	87.4	98.1
2400.0	31.7	40.8	50.1	62.7	79.7	85.6	97.1
3000.0	31.3	41.0	51.0	61.6	86.6	93.5	110.3

TABLE S1

SPRING.30.RMS.2

Baseline, m	Averaging Time, s 30.	60.	120.	240.	480.	960.	3600.
16.0	12.6	13.0	13.3	13.4	13.5	13.5	13.3
24.0	16.0	16.6	16.6	16.7	16.8	17.3	16.9
40.0	22.5	23.2	23.4	23.6	23.7	24.2	23.6
60.0	29.6	30.8	31.4	31.7	31.8	32.1	31.5
84.0	34.9	36.6	37.1	37.7	37.8	38.2	37.5
100.0	37.4	39.5	40.3	41.0	41.2	41.6	40.7
150.0	41.3	45.0	46.7	47.9	48.2	48.7	47.8
210.0	44.3	50.4	53.1	54.6	55.1	55.3	54.7
250.0	44.7	52.2	55.5	57.2	57.8	57.8	57.6
350.0	44.8	55.6	61.0	64.3	65.3	65.3	65.3
400.0	44.4	56.4	62.4	65.9	67.1	66.5	67.7
500.0	42.1	54.9	63.8	68.7	70.6	70.3	71.8
600.0	41.1	53.3	64.9	70.9	73.5	73.2	75.5
700.0	41.4	56.2	67.6	73.9	78.5	77.4	80.0
750.0	41.9	56.0	67.0	75.5	79.0	79.7	82.7
800.0	41.9	56.5	70.5	77.7	79.0	80.9	82.6
900.0	41.6	55.0	66.6	77.2	82.0	84.5	87.7
1000.0	41.1	53.4	66.1	78.2	84.0	87.1	91.0
1200.0	40.8	54.8	67.5	78.0	90.2	92.7	96.8
1400.0	40.9	56.4	70.4	81.2	93.4	99.0	105.4
1600.0	43.0	55.8	71.3	80.8	98.8	102.2	110.7
2000.0	42.4	57.9	71.1	91.9	106.1	112.1	119.8
2200.0	43.4	58.5	73.3	82.9	110.2	116.5	129.3
2400.0	41.6	54.7	68.1	85.3	106.6	113.6	127.2
3000.0	41.1	55.1	69.0	83.3	114.6	122.6	143.2

TABLE 5-1

SPRING.04.RMS.3

Baseline, m	Averaging Time, s 30.	60.	120.	240.	480.	960.	3600.
16.0	1.1	1.1	1.2	1.2	1.2	1.2	1.2
24.0	1.3	1.3	1.3	1.3	1.3	1.4	1.4
40.0	1.8	1.9	1.9	1.9	2.0	2.0	2.0
60.0	2.4	2.5	2.5	2.6	2.6	2.7	2.7
84.0	2.9	3.0	3.1	3.1	3.2	3.3	3.3
100.0	3.1	3.3	3.3	3.4	3.5	3.6	3.6
150.0	3.5	3.8	3.9	4.0	4.2	4.3	4.4
210.0	3.8	4.2	4.4	4.6	5.0	5.0	5.2
250.0	3.9	4.4	4.7	5.0	5.4	5.5	5.8
350.0	3.8	5.1	5.4	5.8	6.5	6.7	7.0
400.0	3.9	4.8	5.5	6.3	7.1	7.2	7.6
500.0	4.0	5.6	6.0	6.8	8.0	8.2	8.8
600.0	3.9	5.7	6.3	7.3	8.8	9.1	10.0
700.0	3.8	5.2	6.9	8.6	10.0	10.3	11.1
750.0	4.0	5.3	6.6	8.4	10.4	10.6	11.8
800.0	3.9	5.1	7.0	9.6	10.7	11.3	12.5
900.0	4.0	5.5	6.9	9.0	11.7	12.0	13.5
1000.0	4.0	5.7	7.1	9.4	12.5	13.0	14.6
1200.0	4.1	5.7	8.9	11.6	14.5	15.1	16.9
1400.0	4.1	6.1	8.6	11.5	15.9	16.6	19.1
1600.0	4.2	5.9	9.8	13.3	17.8	18.6	21.2
2000.0	4.2	6.2	9.7	15.8	20.6	22.1	25.3
2200.0	4.3	6.1	9.9	14.0	21.9	23.3	27.1
2400.0	4.2	6.4	10.5	16.7	23.3	25.1	29.0
3000.0	4.3	6.6	10.3	16.3	26.5	28.8	34.1

SPRING.07.RMS.3

Baseline, m	Averaging Time, s 30.	60.	120.	240.	480.	960.	3600.
16.0	1.5	1.6	1.7	1.7	1.7	1.7	1.7
24.0	1.9	2.0	2.1	2.1	2.1	2.2	2.2
40.0	2.8	3.0	3.1	3.2	3.2	3.3	3.2
60.0	3.7	4.1	4.3	4.4	4.5	4.5	4.5
84.0	4.8	5.3	5.6	5.7	5.8	5.9	5.8
100.0	5.4	6.0	6.3	6.6	6.7	6.7	6.7
150.0	6.5	7.6	8.2	8.6	8.7	8.9	8.8
210.0	7.5	9.1	10.0	10.6	10.9	10.9	11.1
250.0	7.9	9.8	10.9	11.6	12.0	12.0	12.3
350.0	8.3	11.2	12.9	14.1	14.6	14.8	15.1
400.0	8.3	11.6	13.5	14.8	15.5	15.5	16.2
500.0	7.9	11.4	14.3	16.1	17.1	17.3	18.1
600.0	7.8	11.2	14.8	17.2	18.5	18.8	19.9
700.0	7.8	12.0	15.6	17.9	20.1	20.1	21.4
750.0	7.9	12.3	15.6	18.8	20.6	21.3	22.7
800.0	7.8	12.1	17.0	19.6	20.2	21.3	22.6
900.0	7.7	11.9	15.6	19.7	22.1	23.3	25.0
1000.0	7.7	11.3	15.4	20.3	23.1	24.5	26.5
1200.0	7.7	12.1	16.5	20.2	25.4	26.4	28.8
1400.0	7.6	12.6	17.5	21.7	27.2	29.5	32.6
1600.0	8.2	12.4	18.1	21.6	29.2	30.8	34.8
2000.0	8.0	12.8	17.5	25.0	31.5	34.2	38.8
2200.0	8.2	12.7	18.0	22.4	34.0	36.7	42.6
2400.0	7.8	12.0	17.3	23.9	33.3	36.5	43.1
3000.0	7.8	12.4	17.5	23.7	37.2	41.2	50.2

TABLE S2

SPRING.13.RMS.3

Baseline, m	Averaging Time, s 30.	60.	120.	240.	480.	960.	3600.
16.0	5.2	5.3	5.4	5.5	5.5	5.6	5.4
24.0	6.7	6.9	7.0	7.0	7.0	7.3	7.1
40.0	9.6	10.0	10.0	10.1	10.2	10.5	10.1
60.0	13.0	13.5	13.7	13.9	13.9	14.2	13.8
84.0	16.1	16.8	17.0	17.2	17.3	17.6	17.1
100.0	17.5	18.4	18.7	19.0	19.1	19.5	18.9
150.0	19.7	21.4	22.0	22.5	22.7	23.1	22.5
210.0	20.6	23.3	24.3	25.0	25.2	25.4	25.0
250.0	20.5	23.7	25.1	25.8	26.1	26.2	26.0
350.0	20.3	24.9	27.1	28.5	29.0	29.2	29.1
400.0	20.3	25.4	27.8	29.2	29.8	29.8	30.2
500.0	19.0	24.4	27.9	29.9	30.9	30.9	31.6
600.0	18.6	23.7	28.3	30.7	32.1	32.1	33.3
700.0	18.8	24.9	29.4	31.9	34.2	33.8	35.2
750.0	19.1	24.5	29.2	32.6	34.6	35.1	36.6
800.0	19.1	25.1	30.4	33.7	34.4	35.4	36.4
900.0	18.9	24.3	29.1	33.3	35.9	37.3	39.0
1000.0	18.7	23.8	29.1	33.8	36.9	38.5	40.6
1200.0	18.7	24.3	29.5	33.8	39.7	41.1	43.5
1400.0	18.5	24.9	30.5	34.9	41.3	44.1	47.7
1600.0	19.7	25.0	31.1	35.1	44.0	45.9	50.5
2000.0	19.3	25.7	31.2	40.1	47.4	50.7	55.5
2200.0	19.7	26.2	32.3	36.3	50.0	53.3	60.2
2400.0	19.0	24.6	29.9	37.5	48.4	52.4	60.0
3000.0	18.9	24.9	30.6	37.3	53.1	58.0	68.7

SPRING.20.RMS.3

Baseline, m	Averaging Time, s 30.	60.	120.	240.	480.	960.	3600.
16.0	6.4	6.6	6.8	6.9	6.9	6.9	6.8
24.0	8.1	8.5	8.5	8.6	8.6	8.9	8.7
40.0	11.5	12.1	12.2	12.4	12.4	12.7	12.4
60.0	15.4	16.2	16.6	16.9	17.0	17.1	16.8
84.0	18.7	19.9	20.4	20.8	20.9	21.2	20.8
100.0	20.4	22.0	22.6	23.1	23.2	23.5	23.0
150.0	23.3	26.0	27.3	28.1	28.4	28.8	28.3
210.0	25.6	29.8	31.9	33.1	33.5	33.7	33.5
250.0	26.2	31.4	33.9	35.3	35.8	35.9	35.9
350.0	26.7	34.2	38.2	40.8	41.7	41.8	42.0
400.0	26.5	35.0	39.5	42.2	43.3	43.0	44.2
500.0	25.1	34.1	40.8	44.7	46.4	46.4	47.8
600.0	24.5	33.2	41.9	46.8	49.0	49.1	51.1
700.0	24.6	35.2	43.7	48.7	52.6	52.1	54.4
750.0	25.0	35.5	43.5	50.2	53.4	54.3	56.8
800.0	24.9	35.4	46.3	51.9	53.0	54.8	56.6
900.0	24.7	34.5	43.3	51.8	56.1	58.2	61.1
1000.0	24.4	33.3	42.9	52.8	57.8	60.5	64.0
1200.0	24.2	34.6	44.5	52.6	62.7	64.7	68.6
1400.0	24.2	35.9	46.7	55.5	65.8	70.4	75.9
1600.0	25.8	35.4	47.7	55.2	70.1	73.0	80.2
2000.0	25.2	36.7	46.9	63.2	75.4	80.3	87.8
2200.0	25.9	36.8	48.4	56.7	79.4	84.5	95.5
2400.0	24.7	34.5	45.5	59.2	77.1	83.0	95.0
3000.0	24.4	35.1	46.0	58.0	84.1	91.2	108.4

TABLE S2

SPRING.30.RMS.3 Baseline, m	Averaging Time, s 30.	60.	120.	240.	480.	960.	3600.
16.0	7.0	7.3	7.5	7.6	7.6	7.7	7.6
24.0	8.8	9.3	9.4	9.5	9.6	9.9	9.6
40.0	12.7	13.5	13.8	14.0	14.0	14.4	14.0
60.0	17.1	18.4	18.9	19.4	19.5	19.7	19.3
84.0	21.3	23.2	23.9	24.5	24.7	25.0	24.5
100.0	23.6	26.0	26.9	27.7	27.9	28.2	27.6
150.0	27.9	31.8	33.8	35.0	35.4	35.8	35.3
210.0	31.4	37.4	40.5	42.2	42.8	43.0	42.8
250.0	32.6	39.9	43.6	45.7	46.4	46.5	46.6
350.0	33.8	44.4	50.2	53.8	55.1	55.0	55.4
400.0	33.6	45.7	52.2	56.2	57.5	57.0	58.6
500.0	32.1	48.2	57.3	60.3	63.3	62.2	64.4
600.0	31.1	43.6	56.1	63.1	66.0	66.0	68.4
700.0	31.2	46.3	58.8	65.8	70.9	70.1	72.8
800.0	31.4	46.4	62.6	69.9	71.3	73.6	75.7
900.0	31.1	45.4	57.9	70.2	75.5	78.0	81.6
1000.0	30.8	43.4	57.1	71.5	77.8	81.1	85.2
1200.0	30.5	45.7	59.8	71.2	84.1	86.4	91.0
1400.0	30.4	47.4	62.7	75.4	88.2	94.0	100.5
1600.0	32.6	46.4	64.4	75.0	93.7	97.3	105.7
2000.0	31.7	48.2	62.7	85.1	100.4	106.3	114.6
2200.0	32.7	47.9	64.4	76.3	105.0	111.1	124.4
2400.0	31.1	45.1	60.9	79.7	102.0	108.8	123.0
3000.0	30.8	46.0	61.2	77.4	110.0	118.1	139.2

TABLE S2

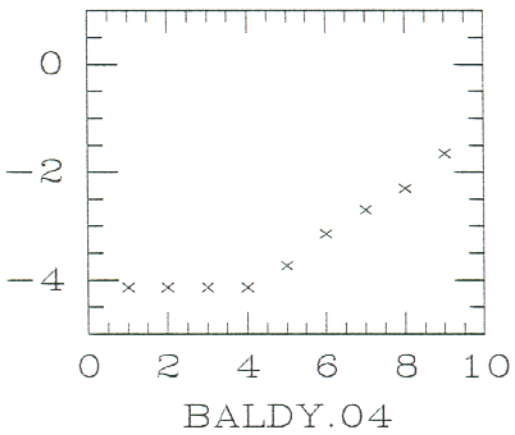

BALDY.04

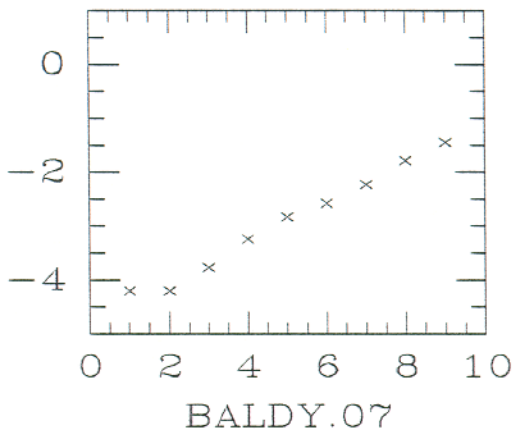

BALDY.07

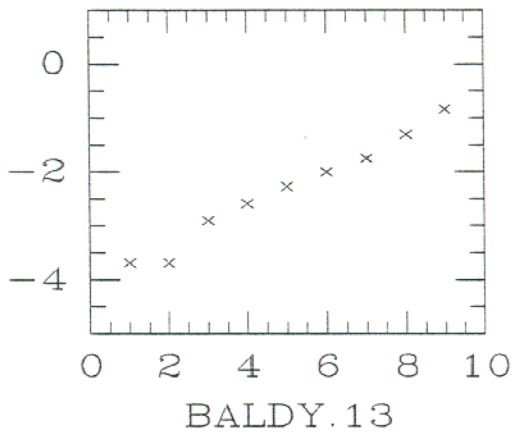

BALDY.13

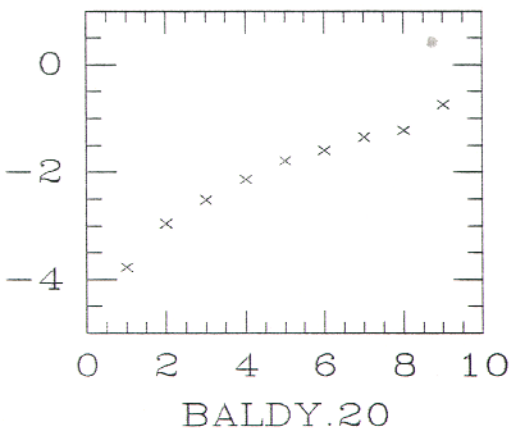

BALDY.20

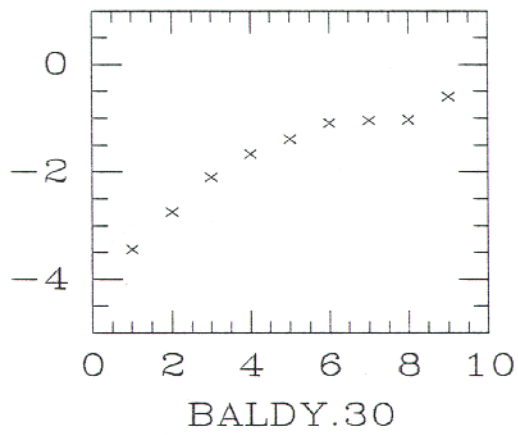

BALDY.30

Truth

Fig 1

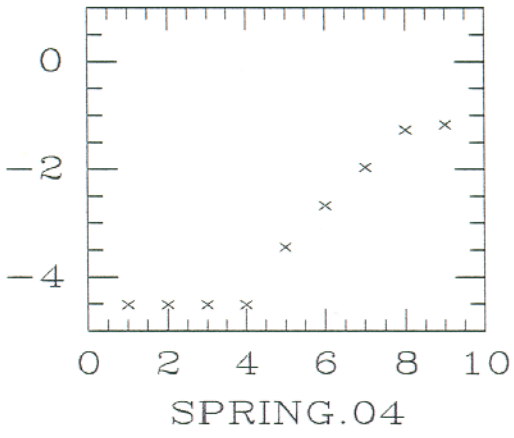

SPRING.04

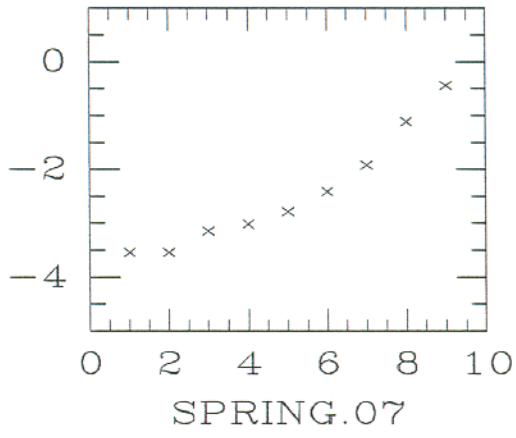

SPRING.07

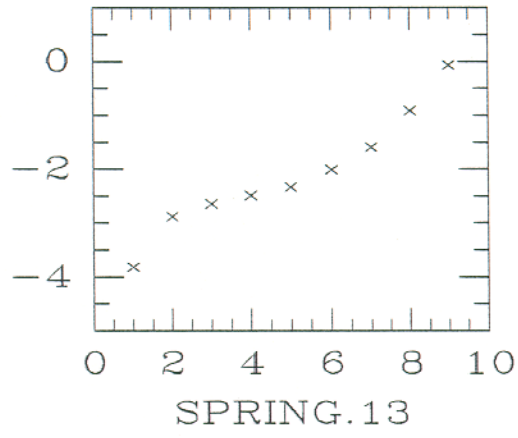

SPRING.13

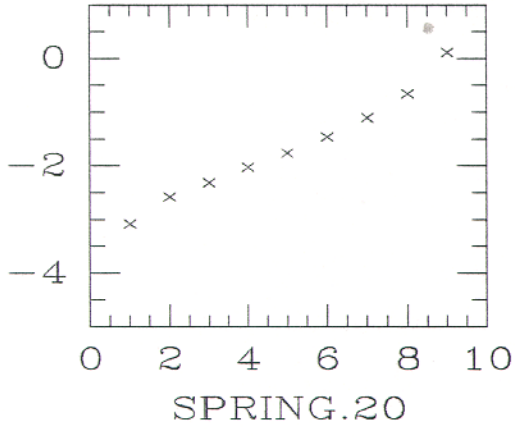

SPRING.20

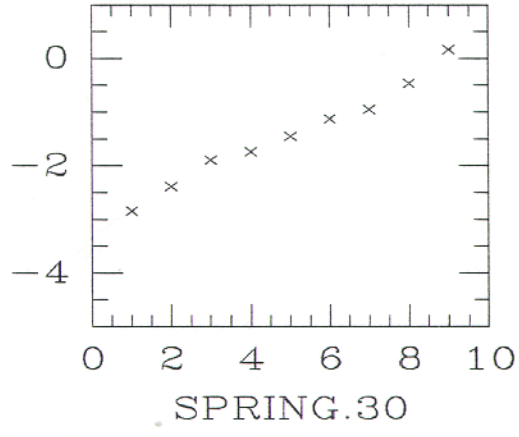

SPRING.30

Truth

Fig 2

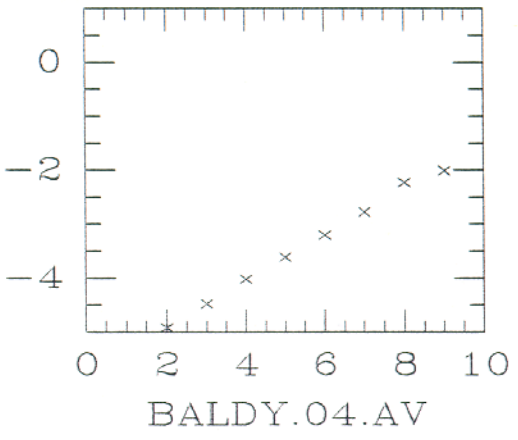
0
−2
−4
0 2 4 6 8 10
BALDY.04.AV

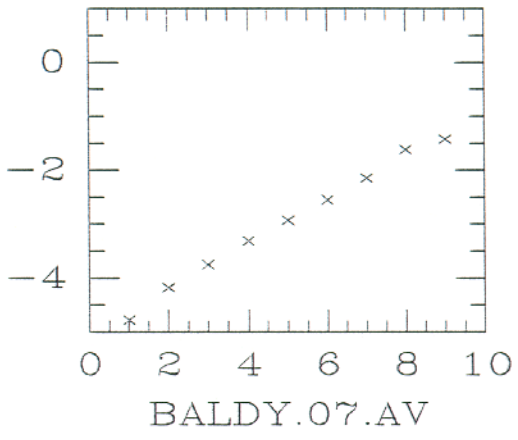
0
−2
−4
0 2 4 6 8 10
BALDY.07.AV

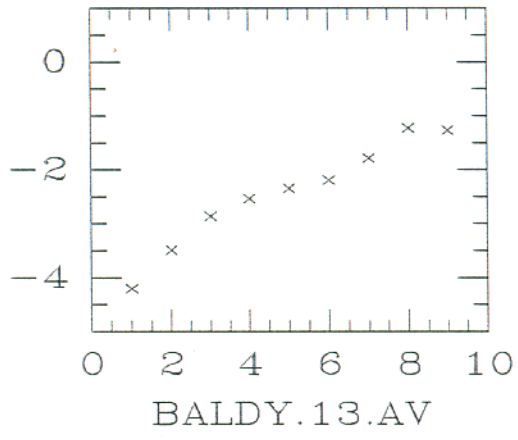
0
−2
−4
0 2 4 6 8 10
BALDY.13.AV

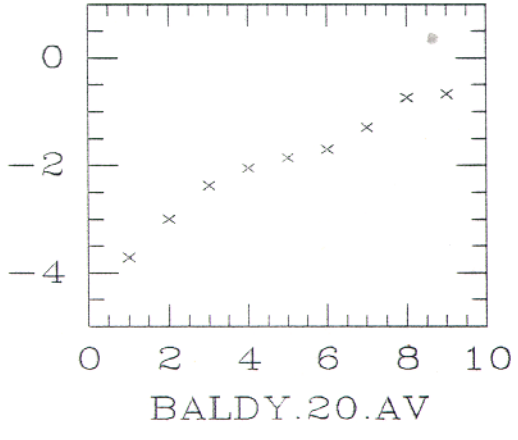
0
−2
−4
0 2 4 6 8 10
BALDY.20.AV

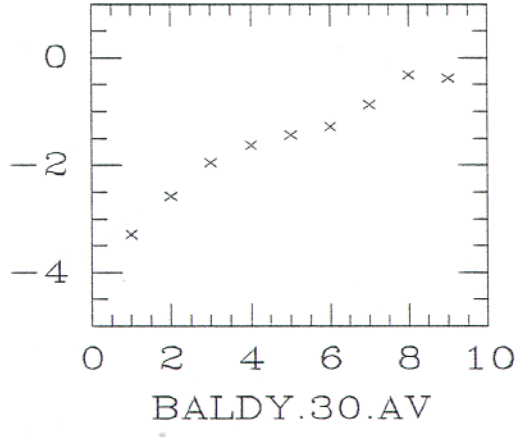
0
−2
−4
0 2 4 6 8 10
BALDY.30.AV

Fig 3

SIM 2

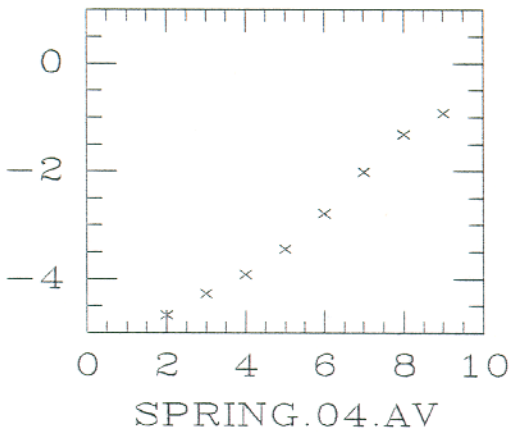
0
−2
−4
0 2 4 6 8 10
SPRING.04.AV

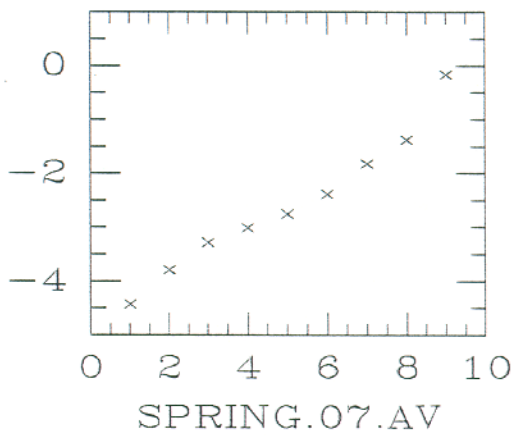
0
−2
−4
0 2 4 6 8 10
SPRING.07.AV

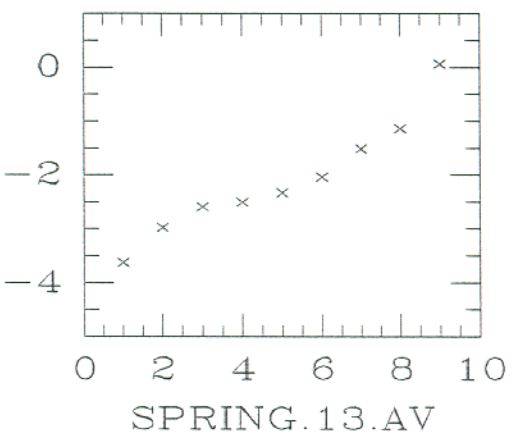
0
−2
−4
0 2 4 6 8 10
SPRING.13.AV

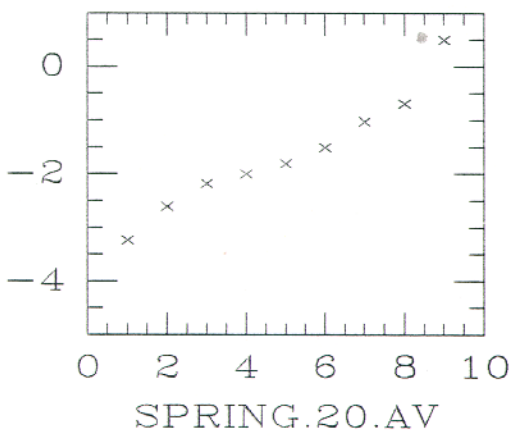
0
−2
−4
0 2 4 6 8 10
SPRING.20.AV

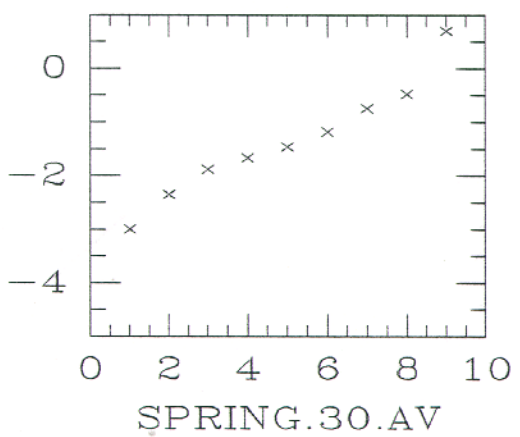
0
−2
−4
0 2 4 6 8 10
SPRING.30.AV

Fig 4

SIM1

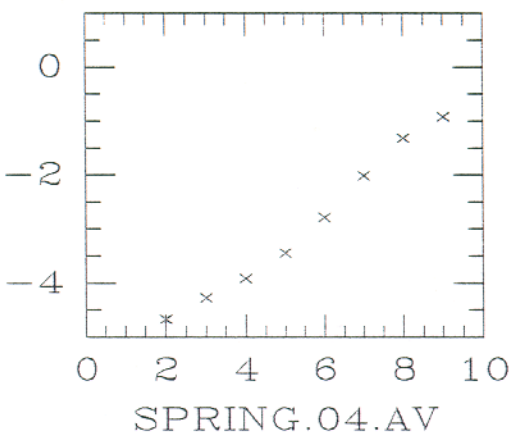
0
−2
−4
0 2 4 6 8 10
SPRING.04.AV

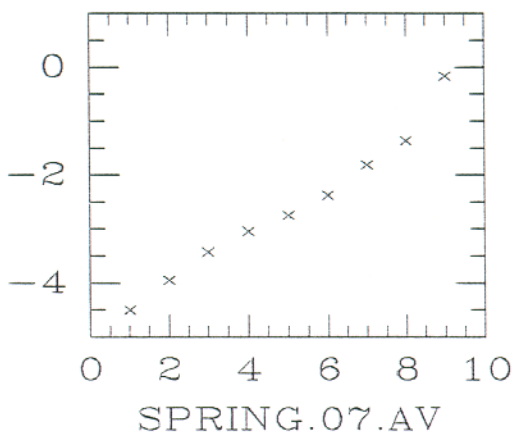
0
−2
−4
0 2 4 6 8 10
SPRING.07.AV

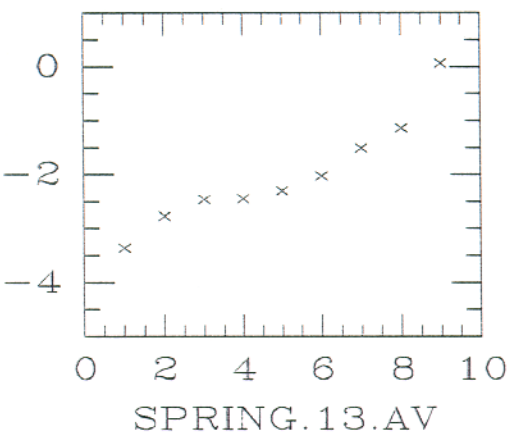
0
−2
−4
0 2 4 6 8 10
SPRING.13.AV

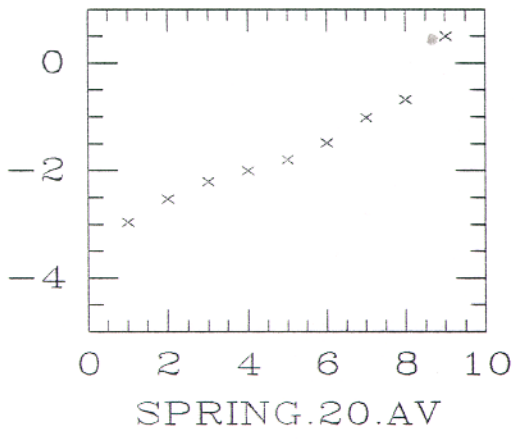
0
−2
−4
0 2 4 6 8 10
SPRING.20.AV

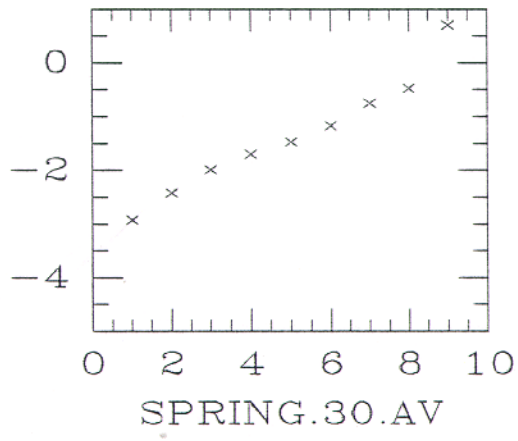
0
−2
−4
0 2 4 6 8 10
SPRING.30.AV

Fig 5

sim 2

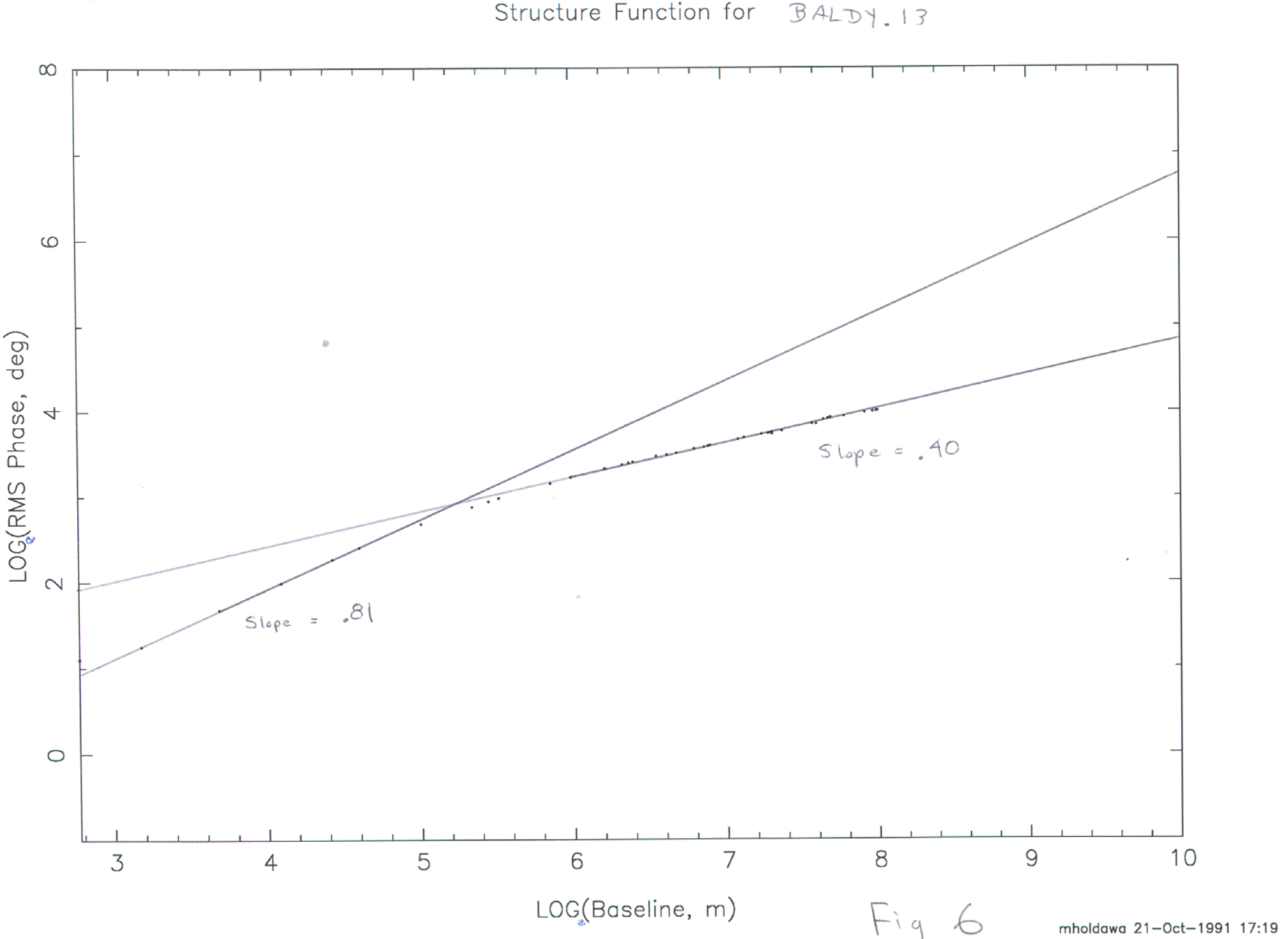

Fig 6

mholdawa 21-Oct-1991 17:19